Egyptian Journal of Chemistry

http://ejchem.journals.ekb.eg/

Studying and Evaluating Catalytic Pyrolysis of Polypropylene

Ameen Abdelrahman[a], Asmaa S. Hamouda[b*], H F M Mohamed[c], A.H. Zaki[d]

[a] *Renewable Energy Science & Engineering Department, Faculty of Postgraduate Studies for Advanced Science, Beni-Suef University, P.O. Box 62511 Beni-Suef, Egypt. E-mail: chem.shaha@hotmail.com*

[b] *Department of Environmental Sciences and Industrial Development, Faculty of Postgraduate Studies for Advanced Sciences, Beni-Suef University, P.O. Box 62511 Beni-Suef, Egypt.*

[c] *Physics Department, Faculty of Science, Minia University, P.O. Box 61519 Minia, Egypt*

[d] *Department of Materials Science and nanotechnology, Faculty of Postgraduate Studies for Advanced Sciences, Beni-Suef University, P.O. Box 62511 Beni-Suef, Egypt*

Abstract

Renewable energy and alternative fuel from different conventional resources such as biomass, plastic waste, and recyclable polymers are impertinent environmental issues worldwide. Furthermore, to replace fossil fuel and reduce greenhouse gas emissions that have a negative impact on climate change. This article exhibits the effect of metal oxide composite/clay in the thermal decomposition of Polypropylene. That hetrocatalyst composed nano-clay thin layer loaded with MnO_2 –NPs works on cracking of polypropylene under different reaction conditions like heating temperature, rate of reaction, reaction time, and composite loading ratio. Various techniques such as GC and TEM were used to characterize pyrolysis gases and char, in addition to scanning electron microscopy (SEM), Fourier transform infrared (FTIR), Thermo-gravimetric analyzer (TGA), and X-ray diffraction (XRD) were used for composite characterize. High gas yield and char rate conversion were obtained using synthesize composite.

Keywords: Clay metal oxides; Nanocomposites; Catalytic thermochemical cracking; Plastic waste; Polypropylene

1. Introduction

The production of alternative fuel from biomass and waste is necessary. The conventional way of plastic recycling or degradation releases harmful gases such as CO, CO_2, and NO_2, and the landfill process pollutes the underground water reservoir. On the other hand, plastic has played a vital role in enhancing the standard of living of human beings for more than 50 years (1). It has led to the innovation of other products used in various sectors such as construction, healthcare, electronics, automation, and packaging. The demand of commodity plastics increased with a rapid increase in the world population owing to its low weight, low cost, flexibility, reusability, anti-rust property, etc. Therefore, global plastic production has increased by almost 10% every year since 1950 (1). In Egypt, the treatment of municipal solid waste has become a great concern. A total of 55 tons of municipal solid waste is generated daily, according to the estimate in 2011 (2). This amounts to 20 million tons of waste annually, and this amount is expected to double increasing by 2022 (2). In Egypt, MSW is 100% recyclable; high-end garbage in Cairo is composed of 65% organic material (leftover vegetables, fruits, bread, and other food scraps and remnants of the kitchen), 15% paper, 3% glass, 3% Plastic, 3% cloth, 1% bone, 1% metals, and 9% other materials (3).

The excessive use of synthetic plastics has led to an increase in plastic waste. Therefore, many countries have prohibited these two treatment technologies and are emphasizing on recycling waste plastics. However, the effective recycling of waste plastics is limited by the economical barrier caused by the low quality of recycled waste plastics (4-8). Among the various types of waste plastics, the conversion of polyethylene (PE) and polypropylene (PP) to proper fuel or chemical feedstock via simple pyrolysis is difficult, because most PE and PP pyrolysis products consist of low-quality wax with a

*Corresponding author e-mail: asmaa_hamouda@psas.bsu.edu.eg , asmaa_hamouda@yahoo.com
Receive Date: 31 October 2020, Revise Date: 20 January 2021, Accept Date: 23 February 2021
DOI: 10.21608/EJCHEM.2021.48239.2988

wide carbon number distribution. Several mechanisms exist for breaking long-chain plastic polymers, such as randomly cutting polymer chains and cutting the end of the chain. A mechanism is chosen on the basis of the covalent bond dissociation energy, degrees of aromatisation, and the presence of halogen and other heteroatoms in the polymer chain (9). Catalytic pyrolysis is a thermochemical conversion route for lignocellulose biomass to produce chemicals and fuels compatible with the current petrochemical infrastructure. Several structures have been used for both thermal and catalytic pyrolysis of waste plastics, such as a tube furnace (10), a batch reactor (11-13), a fixed bed (14-16), a fluidized bed (17-19), and/or a spouted bed (20-23). Pyrolysis in a fluidized bed reactor is the more widely studied technology on a laboratory and pilot plant scale. Plastic pyrolysis in fluidized bed reactors is carried out normally at a temperature as low as 290 °C–850 °C for both thermal and catalytic processes.

Pyrolysis is a form of tertiary recycling carried out in the absence of oxygen, leading to the thermal degradation of the plastic. The mechanism of the process is the cracking of the high-molecular-weight polymer chain to low-molecular-weight hydrocarbon oils and gases. To improve the quality of the product yield and reduce the cost and time consumed, scientists and engineers are trying to explore ideal parameters and material catalysts. Serrano et al. and Aguado et al. (24-25) used zeolites as effective catalysts for upgrading the quality of pyrolysis oil (product). Zeolite catalysts exhibit high catalytic activity, high shape selectivity, strong acidity, and high stability at elevated temperatures.

In recent years, metal nanomaterials have been used as heterogeneous catalysts (26-29). These catalysts have a very high catalytic activity and selectivity for specific reactions. Nanocatalysts have been used in oxidation reactions (26), reduction reactions (27), coupling reactions (28-29), and electrochemical reactions (30-34).

Lin et al. (35) worked towards using catalysts to reduce the required reaction temperature, improve the yield of volatile products, and provide selectivity in the product distributions. Zhao et al. (36) observed that the pyrolysis temperature and the composition of the hydrocarbon product depend on the type of catalyst used. Williams et al. (37) carried out the pyrolysis of polystyrene and found that the concentration of polycyclic aromatic hydrocarbons in the derived pyrolysis oil depends on the type of catalyst used. Mordi et al. (38).Research on using magnesium compounds for fire retardation treatment of wood and other cellulosic materials is scarce. Ondrej Grexa et al. (39) and Kawamoto et al. (40) carried out pyrolysis of $MgCl_2$-treated filter paper and characterized the products. It was found that $MgCl_2$ had a catalytic action at 250 °C on the polymerisation of levoglucosan in cellulose; it reduced the formation of volatile levoglucose and thus decreased the flammable volatile yield. They also found that MgCl2 increased the primary char yield of cellulose heated at 400 °C. Mostashari et al. (41) and Kaixin et al. (42) investigated the catalytic activity of microporous and mesoporous catalysts in the pyrolysis of waste PE and PP mixture in a batch reactor at 500 °C. How to best use this coproduct depends on the local economic circumstances and the char properties. Combustion of char to supply heat is a commonly used method (43-44), while a few chars may be suitable for further activation to be used in higher-value adsorption applications (45, 46). Williams and Slaney (47) have indicated that the pyrolysis oil yield and qualities of high-density PE, low-density PE, and PP depend on the operating pyrolysis conditions. PE and PP decompose to give various paraffin and olefins (48). Also, liquid product yields of PE and PP pyrolysis are higher than 80% at high temperatures. Gaseous product (C2–C4) yields increase and liquid product (C5–C9) yields decrease with an increase in temperature (49).

The waste plastic could be used in pyrolysis process (zero waste) better than incineration process because it is become source of green gases emission. Alternative technologies for managing end-of-life plastics exist. Nano-clay with Mn-oxide is a good catalyst deforming of polymers to produce Pyrogas which can be used in fuel cell and different applications.

2. Experimental

2.1. Materials

Polypropylene (PP) plastic sample used for the process was purchased from Saudi Basic Industries Corporation (SABIC), KSA. Bentonite powder was purchased from M-I SWACO, Egypt. Other chemicals were purchased from Sigma-Aldrich, Egypt.

2.2 Catalyst (MnO_2 preparation).

MnO_2 was prepared via co-precipitation using two anionic Mn-salts, manganese (II) sulphate, and manganese oxalate. The two salts with the same concentration (0.2 M) were mixed with continuous stirring at a constant temperature of 60 °C. During stirring, a sodium hydroxide solution was added to increase the pH of the solution to be 12. A brown precipitate was observed after stirring for 1 h at 60 °C, which was then filtered and washed with ethanol many times. The precipitate was dried at 100 °C

overnight and then kept in a muffle furnace at 500 °C for 4 h.

2.3 Nano powder clay

A nanopowder form of the clay was prepared via physical methods of grinding (RETSCH Planetary Ball Mills Type PM 400). The clay sample was milled for 8 h by using the ball mill at 150 rpm [50, 51]. For the preparation of composite magnesium clay, 1 g of sodium montmorillonite (clay) was dissolved in 250 mL of distilled water and swelled for 48 h. Then, nanoclay was separated by centrifugation and transferred to a suspension solution (0.5 g of MnO2 was dissolved in 50 mL of distilled water) to prepare the nanoclay composite. The mixture was stirred for 24 h and the precipitate was separated by centrifugation, washed with water, and dried under vacuum overnight [52].

2.4 Characterization

The crystalline structure of the nanoclay was detected by X-ray diffraction (XRD). The XRD patterns were recorded with a Pan Analytical Model X' Pert Pro, which was equipped with CuKα radiation (λ = 0.1542 nm), Ni-filter, and a detector. The patterns were recorded in the 2θ range of 0.5°–90° at a step size of 0.03°. Measurements were recorded at Research Central Metallurgical Research and Development Institute, Egypt. Nanostructure size and shape of the prepared samples were detected using transmission electron microscopy (TEM, JEOL JEM-1230). TEM was operated at 120 kV and was connected to a CCD camera. A copper grid was pre-covered with a very thin amorphous carbon film, and small droplets of the suspended sample solution were placed on the carbon-coated grid. In addition, scanning electron microscopy (SEM) measurements were recorded on the SEM model Oxford instrument INCA/Sight at 40 kV. Both TEM and SEM measurements were recorded at the National Research Centre, Egypt.

All Fourier Transform Infrared (FTIR) spectra were investigated using ATI Mattson genesis spectrometer on the range of wavenumber from 4000-500 cm^{-1} with 2 cm^{-1} resolution. The infrared spectroscopic analysis of the prepared polymeric were conducted by Egyptian Petroleum Research Institute, Egypt.

PP char samples extracted from the pyrolysis reactor were analyzed using various techniques, such as elemental analysis (CHNSO elemental, Vario EL III), at the Central Analytical Laboratories of National Research Centre, Egypt, and gas product yields were analyzed using gas chromatography (VARIAN model CP-3800) at the Egyptian Petroleum Research Institute, Egypt.

The thermogravimetric analyses (TGA) of polypropylene have been measured using different heating rates 5, 10, and 20 oC/min. Analysis and characterization have been done at the Petroleum Research Institute, Egypt, using TA Instruments, TGA Q500, which operated masses of a sample between 0-200 mg, 0.1ug sensitivity of accuracy 0.01%, associated temperature controller up to 800°C. The analyses carried out under N2 or air. The device is provided with an autosampler and an EGA type furnace (quartz).

2.5 Pyrolysis system

Pyrolysis of PP was carried out in a bench-scale fixed-bed reactor (SS 316, 0.98 mm ID). The height of the reactor is 38 cm and its volume capacity 42 cm^3, connected by an electrical furnace. The reactor contains three main parts joined together during experiments. PP sample and any additives are added through the lower part. The upper and lower part of the reactor is linked together by a middle fitting connection as shown in Fig. (1). In this study, 1 g of virgin PP sample (with or without additives) was loaded inside the reactor. The non-condensable gases are flashed from the top of the reactor and measured by displacement of water in the gas sampler collector. Also, char and tar are collected and weighted after the reactor was opened.

2.5.1 Pyrolysis procedure

The air in the reactor was purged for at least 5 min using the selected pyrolysis agent (100% nitrogen). The fixed-bed reactor was installed in its place inside the furnace at the selected reaction temperature. A duration of 5–10 min is required to reach isothermal heating. The electrical furnace (60 cm long, 7 cm ID, and 20 cm OD) was insulated with glass wool material to maintain the pyrolysis temperature. Furthermore, the temperature controller was linked with a thermocouple (type K) on the outer surface of the reactor to record and control the temperature inside the reactor. After the completion of pyrolysis, the sample is removed from the reactor and cooled at room temperature. The gases present inside the GS glasses tubes are displaced by adding water, and residual char or coke is collected and weighted [53].

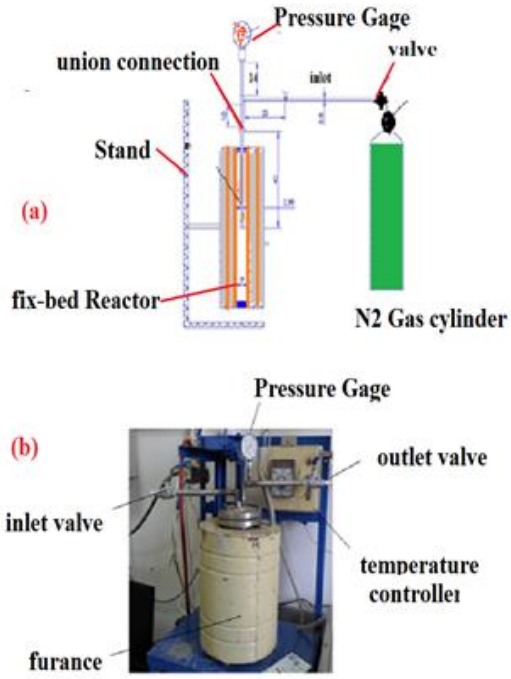

Fig. (1): Pyrolysis system setting up.

3. Results and Discussion

3.1. Physical characterization of virgin PP sample and catalysts.

PP exhibits advantageous properties such as rigidity, heat resistance, saturated linear hydrocarbon chain, and melt more than 160 °C, making it preferable for use in the plastic industry. The widespread applications of PP include the production of a flowerpot, office folders, car bumpers, buckets, carpets, furniture, and storage boxes. It is one of the largest contributors of plastics in municipal solid waste (MSW) [54]. Researchers and scientists [54, 55] have studied the process of pyrolysis of PP by altering various parameters to optimize the liquid oil yield. Ahmad et al. [54] carried out PP pyrolysis at 250 - 400 °C, and 69.82 wt% of liquid oil was achieved at 300 °C. Demirbas [55] conducted pyrolysis of PP at 740 °C in a batch reactor, and 48.8 wt% liquid, 49.6 wt% gas, and 1.6 wt% char yield were obtained. A reduction in liquid and waxes yields were observed with an increase in the pyrolysis temperature.

3.1.1 Proximate and ultimate analysis of virgin PP

The results of the proximate and ultimate analysis of the virgin PP sample are listed in Table (1). The volatile matter obtained after the proximate analysis is 98.83%. Because of the negligible percentage of ash in the virgin PP sample, its degradation happens with minimal formation of the residue. The carbon content after the ultimate analysis is 85.7%. The nitrogen and oxygen contents in the virgin PP sample are not contributed by fillers or impurities but by other ingredients that are added to the resin during the manufacturing of PP.

Table (1). Elemental analysis of the virgin PP sample.

Proximate analysis (wt%)		Elemental composition (wt% on dry ash free)			
Volatile matter	Ash	C	H	N	S
98.83	3.17	85.7	3.5	1.06	0.0

SEM

Morphology of the PP samples was recorded by the SEM instrument operating at 1000× magnification and 10 kV. As seen in Fig. (2), a smooth surface with some fractures spread along the outer surface of the PP sample. Furthermore, SEM examination of the samples shows a near-uniform phase structure with little or no isolated wax phase. Deformation-induced phase segregation is the segregation of a component from a polymer blend due to the application of anisotropic stress and resulting deformation. In this case, the stress takes the form of a compression that permits a sample to deform freely perpendicular to the compression. PP is a highly linear homopolymer that exhibits a series of lamellar stackings that are mostly straight and parallel to each other (although some branching out can be observed) and whose thickness is in the order of 10 nm.

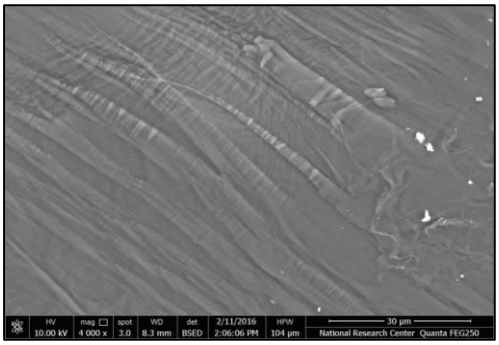

Fig. (2). SEM image of PP sample.

Fourier transform infrared spectrometer (FTIR)

Figure (3) shows the FTIR spectra for the polypropylene sample. The structure of

polypropylene sample various spectrum band wavenumber appears between 750 and 872 cm^{-1} residuals of carbonyl atoms COC of pure PP. Also, the broad peak around 2900 and 2920 cm^{-1} is a good inductor for the CH_3 group of PP. There is another strong peak stretching between 1646.6 and 1731 cm^{-1}, which is evidence for carbonyl group C=O. The functional group, like CH2, vibrated at 2955 and 3000 cm^{-1}. Also, methyl group carbon Skelton CH_3 has a strong peak around 1140, 1194, and 1240 cm^{-1}. On the other hand, symmetry (CH2) is at 2850 cm^{-1}, ν asymmetry (CH_2) is at 2925 cm^{-1}, δ(CH_2) bending is at 1455 cm^{-1}, ν asymmetry (COC) is at 1250 cm^{-1}, and ν symmetry (COC) is at 1045 cm^{-1}.

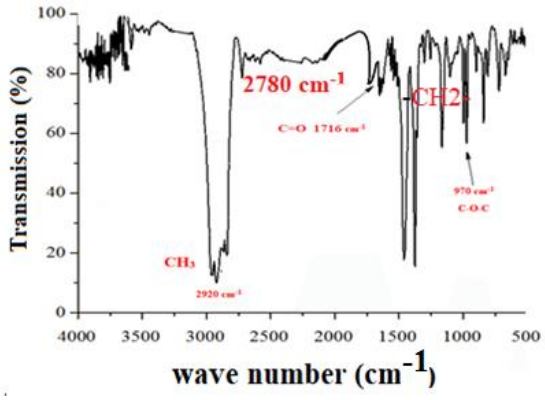

Fig. (3). FTIR spectrum of polypropylene.

TGA

Figure (4) illustrates the thermogravimetric analyses (TGA) of polypropylene using different heating rates 5, 10, and 20 ºC/min. It is clear from the figure that, the degradation PP samples were around 480 to 520 ºC, which is a good indicator for the melting degree Tm. This temperature is the complete conversion of crystalline polymers to liquid and it also will reduce by increasing the heating rate of the pyrolysis system. Also, it due to the lower number of carbon skeleton chains of polymers, which makes it easier to convert to light gases during the oxidation process. On the other hand, setting up optimized parameters was adjustable at 750 ºC, to get rid of wax and liquid tar which is caused the plug of pipe and reactor, moreover erosion of the stainless pipe.

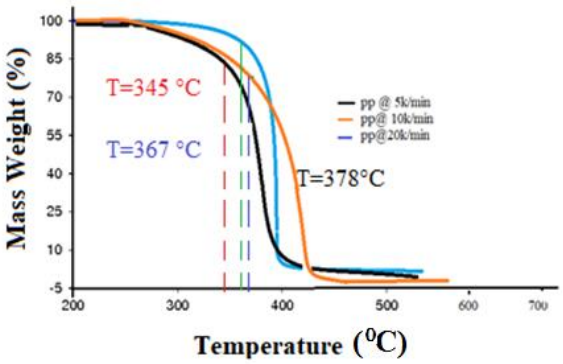

Fig. (4). Mass loss curves of PP at different heating rates.

3.1.2 Characterisation of prepared materials (MnO_2, clay, and composite)

MnO_2 nanostructures such as nanorods, nanowires, and nanofibers have been produced due to their excellent optical, electrical, catalytic, magnetic, and electrochemical properties [57-62]. MnO_2 exists in different structural forms such as α-, β-, γ-, δ-, ε-, and λ-types. The XRD data for all these forms indicate its high crystallinity. The average particle size (d) of the particles was calculated from the high-intensity peak by using the Debye–Scherrer equation as [63]:

$$d = K\lambda/[B \cos(\theta)]. \quad (1)$$

Where K is the Scherrer constant (0.89), λ is the wavelength of the X-ray beam used, B is the full width at half maximum of diffraction (in radians), and θ is the Bragg's angle. Figure 5A shows the XRD pattern of the nanoclay. The shift to lower 2θ values of the (001) and (002) reflections is corresponding to Na+-montmorillonite which can be explained by swelling in the interlamellar space of the clay mineral. Synthesized MnO metal nanoparticles were simply crystalline in nature. The average particle size of the MnO nanoparticles was found to be 25-30 nm. The intensity of the main MnO lines sharply increased, in addition to the appearance of new lines at 2θ angles of 18°, 38°, 43°, and 63° [Fig. (5C)].

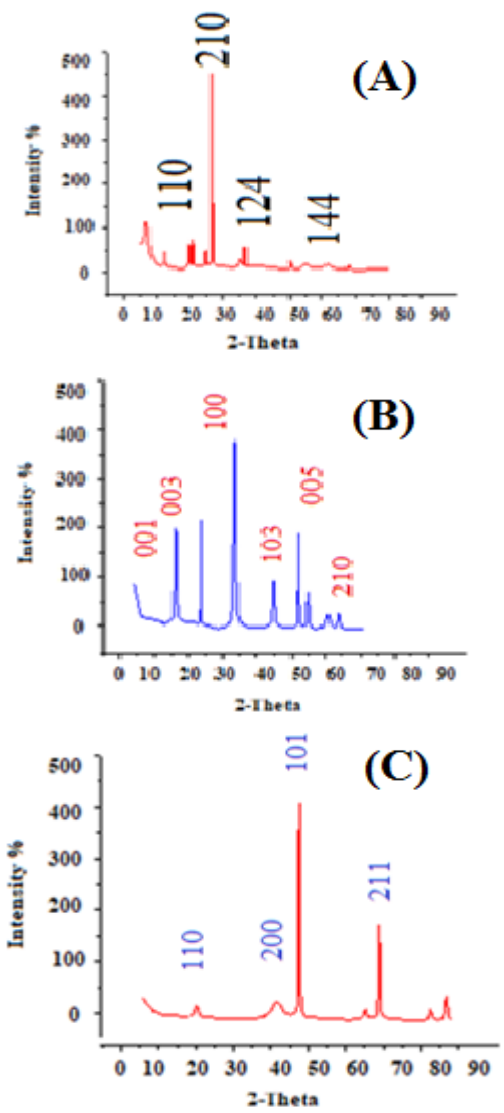

Fig. (5). XRD scans of clay (A), composite (B), and MnO_2 (C).

TEM and SEM

MnO_2 nanoparticles are one of the most attractive inorganic materials because of their physical and chemical properties, leading to their widespread applications in catalysis, ion exchange, and molecular adsorption. It is clear from Fig. (6) that the average size of MnO_2 nanoparticles is about 25-30 nm. MnO_2 nanoparticles have widespread applications, such as catalysts in the cracking of polyolefin and the petroleum refinery industry.

Clay is a montmorillonite mineral species, which belongs to the class of layered smectite clay mineral. Each layer has two tetrahedral sheets containing an octahedral sheet between them. Surface dimensions for one layer are around 300 to more than 600 nm. Hundreds of thousands of these layers are stacked together with van der Waals forces to form clay particles, as shown in Fig. (6b) [25].

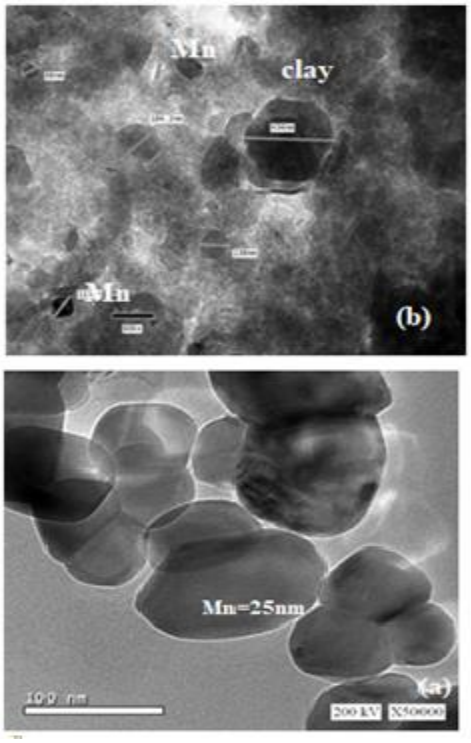

Fig. (6). TEM image of a) MnO_2, and b) Nanometal composite clay

SEM was used to investigate the surface morphologies of the prepared clay- metals composite. Figure 7 shows a massive layered structure with some large flakes and some interlayer spaces. The SEM figure confirms the presence of MnO_2 inside the clay.

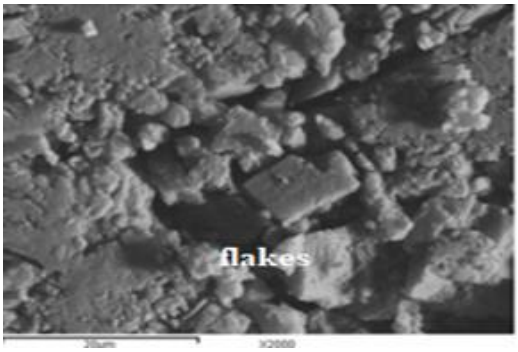

Fig. (7). SEM image of Mn/Clay -composite

3.1.3 Polypropylene Pyrolysis Mechanism

Thermo-catalytically cracking (oxidation) reaction is reverse of the polymerization process, throughout (initiation, propagation, and termination) in presence of a catalyst and O_2 atmosphere addition to raising the temperature. lead to decomposition of polymeric material to hundred of initiative monomers and free radicals' particles such as char (black carbon) and light hydrocarbon components. The mechanism of

pyrolysis includes three-stage. The mechanism of thermal cracking (free radical route, random chain scission) can be depicted as under:

Initiation (thermolysis)

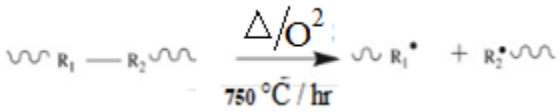

Propagation

A radical may disproportionate thereby forms an olefinic hydrocarbon and a small chain-free radical.

A radical may fragment as under, giving a small chain radical and an aliphatic hydrocarbon:

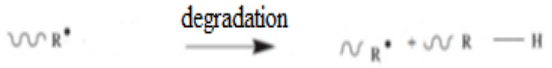

Termination

Hydrogen abstraction (produced by shuttling) leading to the formation of aliphatic hydrocarbons

Retrogressive recombination

char

3.1.4 Kinetic analysis of PP pyrolysis

Considering the TGA results and the weight loss observed over a wide temperature range, the kinetic parameters K_o and E were estimated. The reaction was assumed to be a first-order reaction, and the parameters were estimated according to the following equation as:

$$da/dt = K(1-a) \qquad (2)$$

$$K = K_o \exp(-E_a/RT), \qquad (3)$$

where a = (V* - V/V*) is the percentage of volatile products, K is the Arrhenius kinetic constant, V and V* are the initial and ultimate yields of the volatile products, respectively. E_a is express for the activation energy (J/mol), R is the constant gas value (8.314 J/mol.K), K_o is pre-exponential factor (s^{-1}). The kinetic study was performed in a non-isothermal area of the TGA curves, and the temperature range was from 200 to 500 °C. Usually, the analysis of the differential equation in Eq. (2) leads to Eq. (4), a linearized form from which E_a and Ki are determined:

$$ln\left(-ln\left(\frac{1-x}{T^2}\right)\right) = ln\left(\frac{K_o R}{aE_a}\right) - \frac{E_a}{RT}. \qquad (4)$$

Where E_a is express for the activation energy (J/mol), R is the constant gas value (8.314 J/mol.K), and K_o is the pre-exponential factor (s^{-1}). The plot of $ln\left(-ln\left(\frac{1-x}{T^2}\right)\right)$ versus 1/T is shown in Figure (8-10) ,which is leads to a straight line with slope of $-E_a/R$ and intercept $ln\left(\frac{K_o R}{aE_a}\right)$. So, the activation energy E_a could be calculated from the slope and also the pre-exponential factor could be counted by the intercept.

Temp (ºC)	Temp (K)	1/T	$ln\left(-ln\left(1-\frac{a}{T^2}\right)\right)$	Wt.%
350	623	0.00160571364	-11.164932	99.59
400	673	0.0014858841	-11.558451	98.68
450	723	0.0013831258	-12.486955	86.11
500	773	0.00129366106	-17.562214	1.4

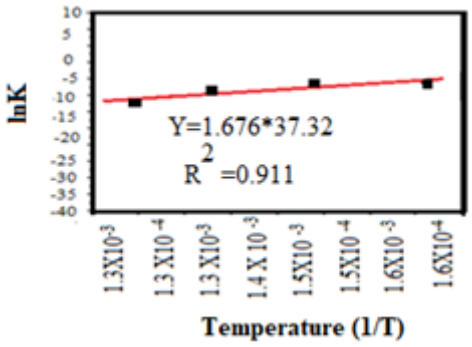

Fig. (8). Thermal decomposition of PP at 5 °C/min.

Temp (ºC)	Temp (K)	1/T	$ln\left(-ln\left(1-\frac{a}{T^2}\right)\right)$	Wt.%
350	623	0.00160571364	-11.281198	99.26
400	673	0.0014858841	-11.922280	95.06
450	723	0.0013831258	-13.349973	56.51
500	773	0.00129366106	-16.952782	2.56

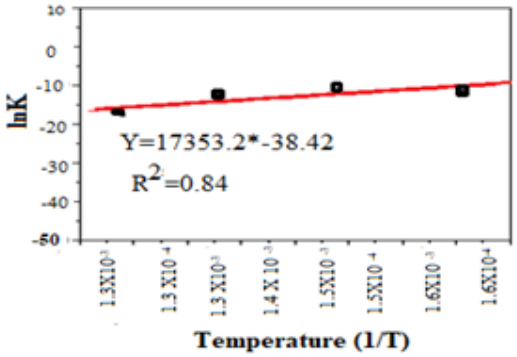

Fig. (9). Thermal decomposition of PP at 10 °C/min.

Temp (ºC)	Temp (K)	1/T	$ln\left(-ln\left(1-\frac{a}{T^2}\right)\right)$	Wt.%
350	623	0.00160571364	-11.562595	97.52
400	673	0.0014858841	-11.823918	96.38
450	723	0.0013831258	-12.633987	81.8
500	773	0.00129366106	-17.636828	1.3

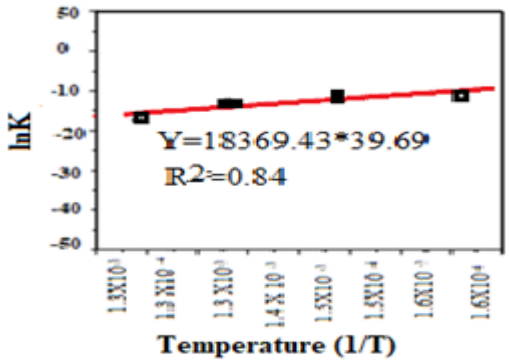

Fig. (10). Thermal decomposition of PP at 20 °C/min.

It is evident from the TGA diagrams that there are two overlapping zones where devolatilization occurs in a temperature range of 200-500 °C for both wastes. The activation energy was found to be 11.3 kcal/mol at 20 °C/min, 54 kcal/mol at 5 °C/min and 77.3 kcal/mol at 10 °C/min. Moreover, the maximum activation energy was observed at 10 °C/min.

For a closer analysis of these thermogravimetric data, the derivative curve of mass loss for all heating rates has been shown in Figure 9. This derivative curve gives a clear picture of any major or sudden loss at specific temperatures. At the heating rate of 50 °C/min, the peak mass loss occurs at 495 °C, with a mass loss rate of 124% mass loss per minute, whereas at the heating rate of 20 °C/min, the peak loss occurs at 487 °C, with a mass loss rate of 57% mass loss per minute.

3.1.5 Optimizing parameters for pyrolysis of PP

Various parameters such as temperature, reaction time, pressure, and catalyst influence the pyrolysis of PP. Temperature is one of the most fundamental operating variables that control the cracking reaction of polymers. Not all polymer materials can be cracked by increasing the temperature, but the thermal cracking of a polymer is changed by changing the temperature, especially in a linear carbon chain. Figure (11) shows different parameterise during of pyrolysis reaction. Homolysis is where the bond breaks so that each fragment has one electron. It reduces its bonding strength due to increasing temperature. Polymer or waste (PP) passes different stages glassy state, rubbery state, liquid state, and decomposition which occurred during the reaction mechanism pyrolysis process: initiation, propagation, hydrogen transfer, and termination reactions referred to previous mechanism scheme. In this study, the optimum temperature for PP degradation was found to be 750 °C because getting of liquid or waxes which deposit on side of the reactor and plugging inlet of reactor, in addition to completely cracking for polymer and conversion gases like carbon mono and dioxide to solid-state char or coke, that is mean decrease emission of carbon dioxide. high value of gas yield and avoid waxes and solid which causes plug for reactor tube by regarding to Figure 11a, b. Reaction time is another factor that affected the reaction in the presence of the catalyst, which was working towards decreasing the activation energy. The optimum reaction time required for the complete pyrolysis of PP is 60 min at 750 °C.

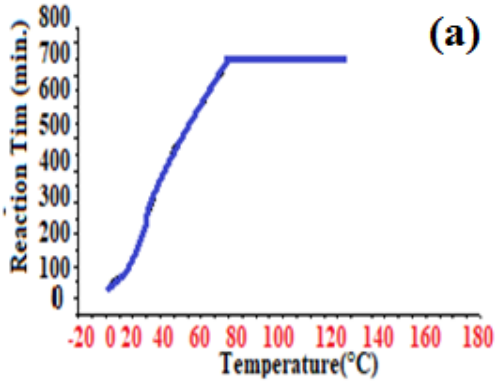

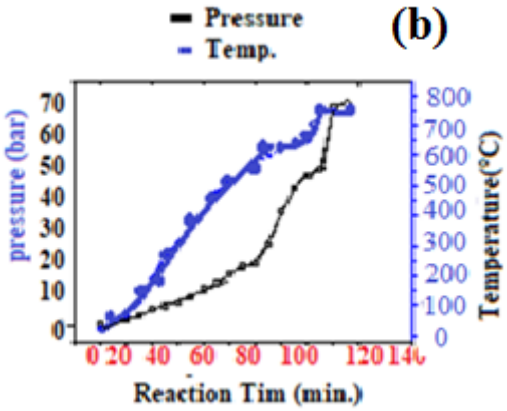

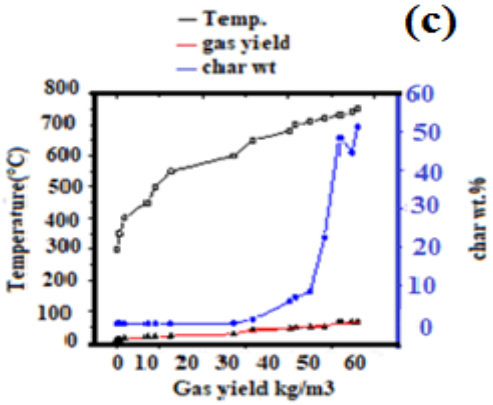

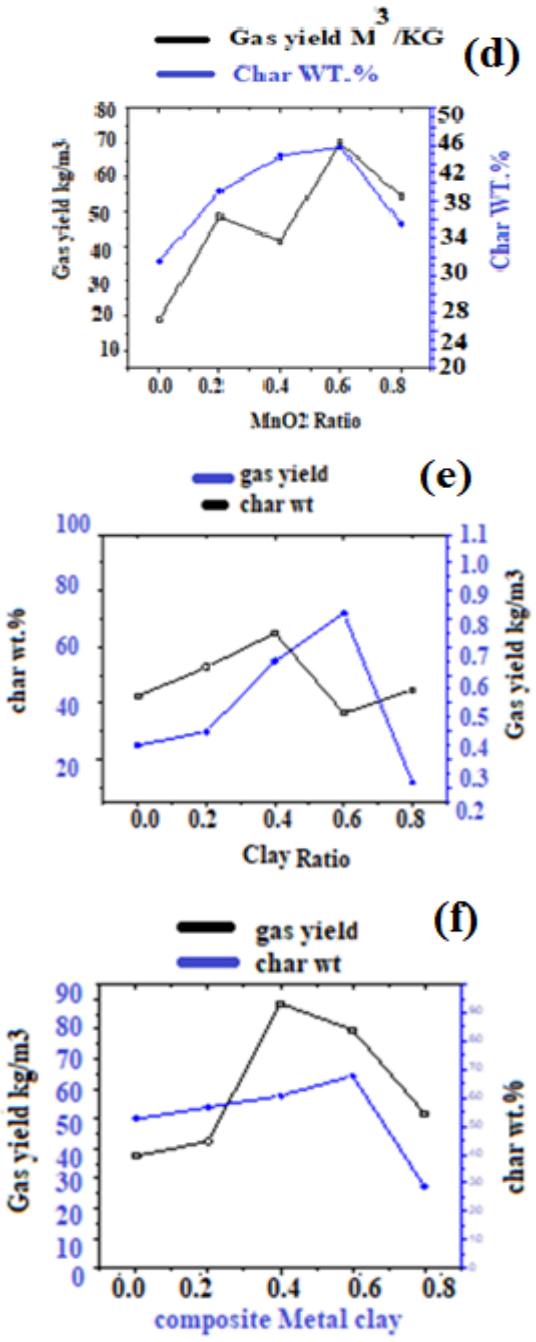

Fig. (11). Different parameterise during of pyrolysis reaction.

As mentioned, a catalyst is one of the important parameters that play a vital role in pyrolysis; it decreases the activation energy and accelerates the reaction by forming and breaking bonds. Clay, MnO_2, and their composite made by adding varying amounts of the catalyst (0, 0.2, 0.4, 0.6, and 0.8%) were used and obtain satisfactory results by using only clay. It was observed that 0.6% of catalyst resulted in 69.8% gas yield and 45.8% of char (coke) compared to other loading amounts of the catalyst [Fig. (10c, e)]. When using clay as a catalyst, we found satisfactory results of cracking (degradation) of PP at the same loaded amount. Furthermore, by increasing the catalyst amount from 0 to 0.6%, the gas yield directly increased from 0.35 to 0.82 and then decreased to 0.22, indicating that the optimum amount of catalyst required for pyrolysis of PP is 0.6%; in addition, 36.5% char is obtained [Fig. (11d, f)]. When using a composite of MnO_2 and clay as a catalyst, it noticed that 0.6 and 0.4% of the composite catalyst gave better gas yields of 79.8 and 88.6, respectively; in addition, 67.8 and 60.8 of char were obtained, respectively, indicating a complete conversion of PP to give by-products.

3.2 studying and evaluation composite effect on pyrolysis products distribution.

3.2.1 Gas yield product.

Breakdown of the polymer chain (PP) gave hundreds of light compounds, gases, liquids, and waxes. Even though we design our parameters to get off the liquid and waxes compound. Throughout these compounds, the efficiency of the catalyst was measured according to the values of those compounds like methane, benzene, hydrogen, and carbon dioxide. The results are shown in Figs. (12-14). Regard previous experiments and data, the best ratio of loading composite works (at a temperature of 750 °C and a time duration of 60 min) to degrade PP pyrolysis is 0.6% wt of the sample. Another evidence, regard to the figures, the best gas yield ratio was obtained using also that amount 0.06% wt of catalyst, in addition, the highest amount of methane is formed by using the same ratio of clay catalyst. Similarly, the highest amounts of hydrogen and CO_2 are formed at 0.6% loading of the clay catalyst. When using MnO_2 as the catalyst, all compounds (methane, hydrogen, and CO_2) were obtained in high yields at 0.6% loading of the catalyst. The electronic configuration of Mn is [Ar]3d54s2, with a half-full d-orbital, which enables it to react. On the other hand, when using composite as the catalyst, similar results were obtained [Fig. (14)].

Catalytical clay ratio, %	(Mol. %)			
	Methane	Hydrogen	Benzene	CO_2
0	79.2	2.1	0.19	1.18
0.2	77.5	1.9	0.448	1.23
0.4	77.9	2.6	0.294	0.99
0.6	82.61	2.81	0.16	1.54
0.8	76.7	2.5	0.19	1.6

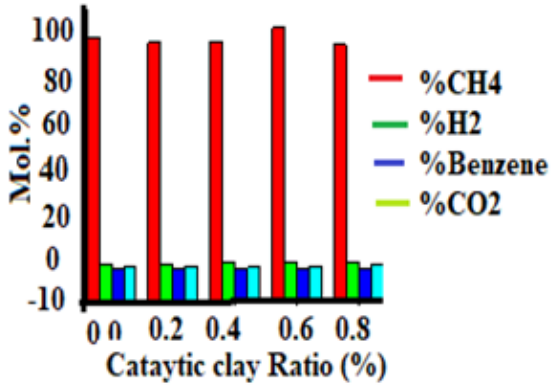

Fig. (12). Gas analysis of PP at 750 °C for 60 min (clay is the catalyst).

Catalytical clay MnO_2, %	(Mol. %)			
	Methane	Hydrogen	Benzene	CO_2
0	75.2	1.9	0.15	1.3
0.2	81.05	2.3	0.18	2.4
0.4	79.9	1.6	0.24	0.99
0.6	84.19	3.79	0.19	2.47
0.8	84.7	1.5	0.166	1.9

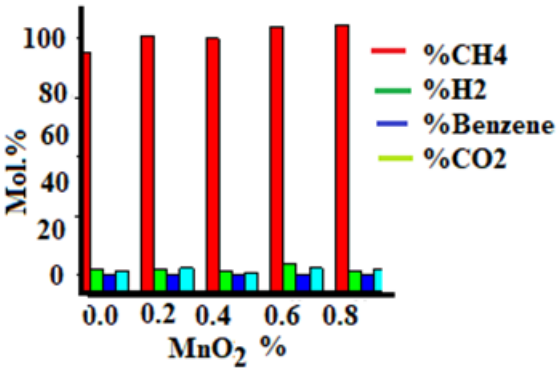

Fig. (13). Gas analysis of PP at 750 °C for 60 min (MnO_2 is the catalyst).

Composite ratio (%)	Methane	Hydrogen	Benzene	CO_2
0	74.6	2	0.22	1.5
0.2	77.6	1.6	0.13	2.4
0.4	80.2	2.3	0.27	2.6
0.6	88.5	2.2	0.24	2.3
0.8	81.7	1.4	0.26	2.1

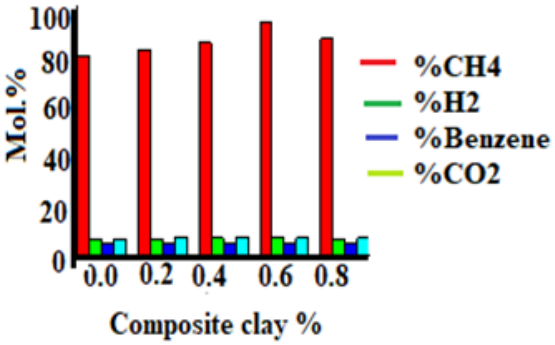

Fig. (14). Gas analysis of PP at 750 °C for 60 min (composite metal clay is the catalyst).

3.2.2 Char characterisation

The surface morphology of pyrolytic char obtained under optimum conditions (0.6% of catalyst at 750 °C for 60 min) is shown in Fig. (15). Many flacks and doping areas (of the size of around 100-120 nm) are seen on the surface of the char sample char, which is evidence of the presence of the metal clay composite submersed in carbon char.

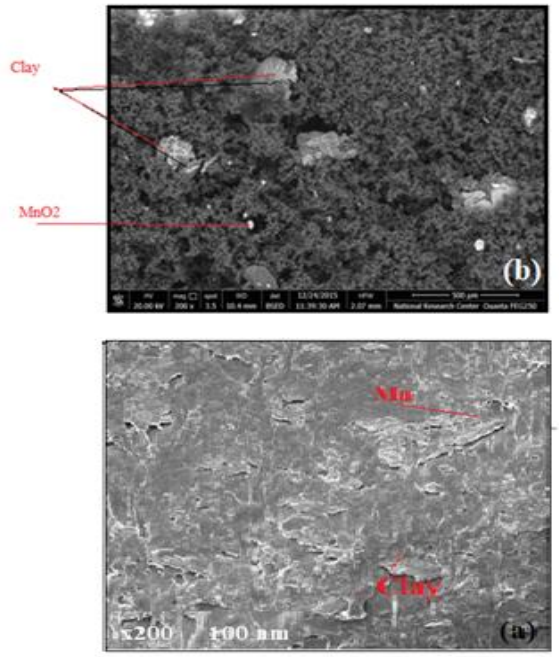

Fig. (15). The surface morphology of pyrolytic char.

Table (3) lists the elemental analysis results for char samples at different loaded catalyst amounts. It is noticed that there are differences in the composition of the main elements (C, H, N, and S). Also, the rate of pyrolytic degradation depends on the amount of catalyst added. Furthermore, in the case of composite, the conversion to carbon is greater than others. Also, the source of N element (trace amount) might be contamination or additives added during the production.

Table (3). Elemental analysis for carbon char after pyrolysis at different reaction rates.

Chemical compositions	N, %	C, %	S, %	H, %
Virgin PP sample	Nil	82.35	Nil	27.85
Carbon char of PP & MnO_2	Nil	69.4	Nil	3.2
Carbon char of PP & clay	Nil	55.70	Nil	1.0
Carbon char of PP & composite	0.71	73.47	Nil	0.85

4. Conclusions

A composite compound from clay and MnO2 was fabricated and characterized. Furthermore, catalytic pyrolysis over thermal pyrolysis was performed. The catalytic pyrolysis leads to the complete degradation of waste plastics to give gases and coke without the formation of liquids or asphaltic materials, which cause problems such as corrosion, line plugging, and reactor damage. Increasing the temperature slightly can eliminate the formation of by-products such as waxes and asphaltic compounds). In addition, the reaction time is directly proportional to temperature and inversely proportional to catalytic activity. The heating rate has less effect on the activation energy under the conditions applied in the study. The pyrolysis of PP was carried out under a different loading of catalysts and the best results (gas yield and char) were obtained at 0.6% loading of catalyst. Gases such as methane and hydrogen were released during the degradation of PP. This is one way the municipal management can eliminate waste plastic by recycling it to produce a useful product by using an economic product (catalyst), which is a green environmental material and is commonly available. Furthermore, CO2 released during the pyrolysis can keep the underground water reservoir in check.

Conflicts of interest

There are no conflicts to declare.

Acknowledgments

This research was supported by the Academy of Scientific Research and Technology "ASRT" as a joint research grant under the India-Egypt agreement on science and technology cooperation. We thank our colleagues from National Research Center who provided us both of pyrolysis reactor system and experience in their laboratory. Prof. Mohamed Abdel Fatah Hamed and Prof. Ali Radwan that greatly assisted the research.

References

[1] Van de Graaf, Thijs. "International Energy Agency." In Handbook of Governance and Security. Edward Elgar Publishing, (2014).

[2] Khodair, Amany. "Evaluating international sources and environmental public policy in Egypt: the case of solid waste management." Public Policy and Administration Research, ISSN: 2224-5731, (2015).

[3] El Gazzar, Rasha Fahim, and Bakr Gomaa. "Municipal Waste Management in Egypt: An Investigation Study of Collection and Generation Process in Alexandria City, Egypt." Red 450: 0-16. (2014).

[4] Han, Tae Uk, Young-Min Kim, Atsushi Watanabe, Norio Teramae, Young-Kwon Park, and Seungdo Kim. "Pyrolysis kinetic analysis of poly (methyl methacrylate) using evolved gas analysis-mass spectrometry." Korean .J .chem.Eng. 34, no. 4: 1214-1221: (2017).

[5] Upare, D. P., Park, S., Kim, M. S., Kim, J., Lee, D., Lee, J., ... & Lee, C. W. Cobalt promoted Mo/beta zeolite for selective hydrocracking of tetralin and pyrolysis fuel oil into monocyclic aromatic hydrocarbons. J Ind Eng Chem, 35, 99-107. (2016).

[6] Al-Salem, S. M., Antelava, A., Constantinou, A., Manos, G., & Dutta, A. (2017). A review on thermal and catalytic pyrolysis of plastic solid waste (PSW). Journal of Environmental Management, 197, 177-198.

[7] Parthasarathy, P., Choi, H. S., Park, H. C., Hwang, J. G., Yoo, H. S., Lee, B. K., & Upadhyay, M. Influence of process conditions on product yield of waste tyre pyrolysis-A review. 2016 *Korean .J .chem.Eng*, 33(8), 2268-2286. (2016).

[8] Yang, W. S., Lee, J. E., Seo, Y. C., Lee, J. S., Yoo, H. M., Park, J. K., ... & Kim, W. H. Utillization of automobile shredder residue (ASR) as a reducing agent for the recovery of black copper. Korean Journal of Chemical Engineering, 33(4), 1267-1277. (2016).

[9] Scheirs, J., and W. Kaminsky. "Converting waste plastics into diesel and other fuels." Feedstock Recycling and Pyrolysis of Waste Plastics; Scheirs, J., Kaminsky, W., Eds (2006)..

[10] Park, Sang Shin, Dong Kyun Seo, Sang Hoon Lee, Tae-U. Yu, and Jungho Hwang. "Study on

pyrolysis characteristics of refuse plastic fuel using lab-scale tube furnace and hermogravimetric analysis reactor." Journal of analytical and applied pyrolysis 97: 29-38. (2012).

[11] Sakata, Y., Uddin, M. A., & Muto, A. Degradation of polyethylene and polypropylene into fuel oil by using solid acid and non-acid catalysts. Journal of analytical and Applied Pyrolysis, 51(1-2), 135-155. (1999).

[12] Zhang, Xuesong, Hanwu Lei, Gayatri Yadavalli, Lei Zhu, Yi Wei, and Yupeng Liu. "Gasoline-range hydrocarbons produced from microwave-induced pyrolysis of low-density polyethylene over ZSM-5." Fuel 144: 33-42. (2015)

[13] Uemura, Y., Baba, K., Ohe, H., Ohzuno, Y., & Hatate, Y. Catalytic decomposition of hydrocarbon into hydrogen and carbon in a spouted-bed reactor as the second-stage reactor of a plastic recycling processJ. Mater. Cycles Waste Manag. , 5(2), 94-97. (2003).

[14] Murata, Katsuhide, Y. Hirano, Y. Sakata, and Md Azhar Uddin. "Basic study on a continuous flow reactor for thermal degradation of polymers." *J. Anal. Appl. Pyrolysis* 65, no. 1: 71-90. (2002) .

[15] Williams, E. A., & Williams, P. T.. The pyrolysis of individual plastics and a plastic mixture in a fixed bed reactor. Journal of Chemical Technology & Biotechnology: International Research in Process, Environmental AND Clean Technology, 70(1), 9-20. (1997).

[16] Aguado, J., Serrano, D. P., Escola, J. M., & Peral, A.. Catalytic cracking of polyethylene over zeolite mordenite with enhanced textural properties J. Anal. Appl. Pyrolysis , 85(1-2), 352-358. (2009).

[17] Kaminsky, W., Predel, M., & Sadiki, A. Feedstock recycling of polymers by pyrolysis in a fluidised bed. Polym. Degrad. Stab. 85(3), 1045-1050. (2004).

[18] Jung, S. H., Cho, M. H., Kang, B. S., & Kim, J. S. Pyrolysis of a fraction of waste polypropylene and polyethylene for the recovery of BTX aromatics using a fluidized bed reactor. Fuel Process. Technol. 91(3), 277-284. (2010).

[19] Luo, G., Suto, T., Yasu, S., & Kato, KCatalytic degradation of high density polyethylene and polypropylene into liquid fuel in a powder-particle fluidized bed. Polym. Degrad. Sta, 70(1), 97-102. (2000).

[20] Elordi, G., Olazar, M., Lopez, G., Artetxe, M., & Bilbao, J. (2011). Product yields and compositions in the continuous pyrolysis of high-density polyethylene in a conical spouted bed reactor. Ind. Eng. Chem 50(11), 6650-6659. (2011).

[21] Artetxe, M., Lopez, G., Amutio, M., Elordi, G., Olazar, M., & Bilbao, J. Operating conditions for the pyrolysis of poly-(ethylene terephthalate) in a conical spouted-bed reactor. Ind. Eng. Chem , 49(5), 2064-2069. (2010).

[22] Aguado, Roberto, Martín Olazar, María J. San José, Beatriz Gaisán, and Javier Bilbao. "Wax formation in the pyrolysis of polyolefins in a conical spouted bed reactor." Energy & fuels 16, no. 6 1429-1437. (2002).

[23] Arabiourrutia, M., Elordi, G., Lopez, G., Borsella, E., Bilbao, J., & Olazar, M.. Characterization of the waxes obtained by the pyrolysis of polyolefin plastics in a conical spouted bed reactor. Anal. Appl. Pyrolysis, 94, 230-237. (2012).

[24] Serrano, D. P., Aguado, J., & Escola, J. M. Developing advanced catalysts for the conversion of polyolefinic waste plastics into fuels and chemicals. ACS Catalysis, 2(9), 1924-1941. (2012).

[25] Aguado, J., Serrano, D. P., & Escola, J. M. Fuels from waste plastics by thermal and catalytic processes: a review. Ind. Eng. Chem., 47(21), 7982-7992. (2008).

[26] Kumar Dutta, D., Jyoti Borah, B., & Pollov Sarmah, P. Recent advances in metal nanoparticles stabilization into nanopores of montmorillonite and their catalytic applications for fine chemicals synthesis. Catal.., 57(3), 257-305. (2015).

[27] Yasukawa, Tomohiro, Aya Suzuki, Hiroyuki Miyamura, Kohei Nishino, and Shū Kobayashi. "Chiral metal nanoparticle systems as heterogeneous catalysts beyond homogeneous metal complex catalysts for asymmetric addition of arylboronic acids to α, β-unsaturated carbonyl compounds." J. Am. Chem. Soc 137, no. 20: 6616-6623. (2015)

[28] Zhang, S., Shen, X., Zheng, Z., Ma, Y., & Qu, Y.. 3D graphene/nylon rope as a skeleton for noble metal nanocatalysts for highly efficient heterogeneous continuous-flow reactions., J. Mater. Chem 3(19), 10504-10511. (2015)

[29] Zhang, S., Li, J., Gao, W., & Qu, Y. (2015). Insights into the effects of surface properties of oxides on the catalytic activity of Pd for C–C coupling reactions. Nanoscale, 7(7), 3016-3021.Zhou W, Zhou Z, Song S, Li W, Sun G, Tsiakaras P and Xin Q 2003 *Appl. Catal. B.* **46** 273 (2015).

[30] Tripković, Amalija V., K. Dj Popović, Branimir N. Grgur, B. Blizanac, P. N. Ross, and N. M. Marković. "Methanol electrooxidation on supported Pt and PtRu catalysts in acid and

alkaline solutions." Electrochimica Acta 47, no. 22-23 : 3707-3714. (2002).
[31] Rees, Neil V., and Richard G. Compton. "Sustainable energy: a review of formic acid electrochemical fuel cells." J SOLID STATE ELECTR 15, no. 10: 2095-2100. (2011).
[32] Shen, Y., Xiao, K., Xi, J., & Qiu, X. Comparison study of few-layered graphene supported platinum and platinum alloys for methanol and ethanol electro-oxidation. J. Power Sources , 278, 235-244. (2015).
[33] Gong, Liyuan, Zhiyuan Yang, Kui Li, Wei Xing, Changpeng Liu, and Junjie Ge. "Recent development of methanol electrooxidation catalysts for direct methanol fuel cell." J. Energy Chem 27, no. 6 : 1618-1628. (2018).
[34] Manos, G., Garforth, A., & Dwyer, J. Catalytic degradation of high-density polyethylene on an ultrastable-Y zeolite. Nature of initial polymer reactions, pattern of formation of gas and liquid products, and temperature effects. Ind. Eng. Chem 39(5), 1203-1208. (2000).
[35] Zhao, Wenwei, Shin Hasegawa, Jun Fujita, Fumio Yoshii, Takashi Sasaki, Keizo Makuuchi, Jiazhen Sun, and Sei-ichi Nishimoto. "Effects of zeolites on the pyrolysis of polypropylene." Polymer degradation and stability 53, no. 1: 129-135. (1996).
[36] Williams, Paul T., Patrick A. Horne, and David T. Taylor. "Polycyclic aromatic hydrocarbons in polystyrene derived pyrolysis oil." J Anal Appl Pyrolysis 25: 325-334. (1993).
[37] Mordi, Raphael C., John Dwyer, and Roy Fields. "H-ZSM-5 catalysed degradation of low density polyethylene, polypropylene, polyisobutylene and squalane: Influence of polymer structure on aromatic product distribution." Polym. Degrad. Stab 46, no. 1 57-62. (1994).
[38] Grexa, Ondrej, Elena Horváthová, and Peter Lehocký. "Flame retardant treated plywood." Polym. Degrad. Stab 64, no. 529-533. 3 (1999).
[39] Kawamoto, Haruo, Daisuke Yamamoto, and Shiro Saka. "Influence of neutral inorganic chlorides on primary and secondary char formation from cellulose." J WOOD SCI 54, no. 3: 242-246. (2008).
[40] Mostashari, S., & Moafi, H.. Thermal decomposition pathway of a cellulosic fabric impregnated by magnesium chloride hexahydrate as a flame-retardant. J. Therm. Anal. Calorim, 93(2), 589-594. (2008)
[41] Li, K., Lee, S. W., Yuan, G., Lei, J., Lin, S., Weerachanchai, P., ... & Wang, J. Y. Investigation into the catalytic activity of microporous and mesoporous catalysts in the pyrolysis of waste polyethylene and polypropylene mixture. Energies, 9(6), 431. (2016).
[42] Boateng, A. A. Characterization and thermal conversion of charcoal derived from fluidized-bed fast pyrolysis oil production of switchgrass. Ind. Eng. Chem. Res, 46(26), 8857-8862. (2007).
[43] Boateng, Akwasi A., Charles A. Mullen, Neil Goldberg, Kevin B. Hicks, Hans-Joachim G. Jung, and JoAnn FS Lamb. "Production of bio-oil from alfalfa stems by fluidized-bed fast pyrolysis." “Ind. Eng. Chem. Res.” 47, no. 12 4115-4122. (2008).
[44] Fan, M., W. Marshall, D. Daugaard, and R. C. Brown. "Steam activation of chars produced from oat hulls and corn stover." Bioresour. Technol 93, no. 1: 103-107. (2004)
[45] Azargohar, R., & Dalai, A. K. Steam and KOH activation of biochar: Experimental and modeling studies. Microporous and Mesoporous Materials, 110(2-3), 413-421. (2008).
[46] Burlakovs, J., Kriipsalu, M., Porshnov, D., Jani, Y., Ozols, V., Pehme, K. M., ... & Klavins, M. Gateway of landfilled plastic waste towards circular economy in Europe. Separations, 6(2), 25. (2019).
[47] Miandad, R., Barakat, M. A., Aburiazaiza, A. S., Rehan, M., Ismail, I. M. I., & Nizami, A. S. Effect of plastic waste types on pyrolysis liquid oil. Int. Biodeterior. Biodegradation” 119, 239-252. (2017).
[48] Demirbas, Ayhan. "Pyrolysis of municipal plastic wastes for recovery of gasoline-range hydrocarbons." “J Anal Appl Pyrolysis”. 72, no. 1: 97-102. (2004).
[49] Xiao, Rui, Baosheng Jin, Hongcang Zhou, Zhaoping Zhong, and Mingyao Zhang. "Air gasification of polypropylene plastic waste in fluidized bed gasifier." “Energy Convers. Manag.” 48, no. 3: 778-786. (2007).
[50] Azzam, E. M. S., Sami, R. M., & Kandile, N. G. Activity inhibition of sulfate reducing bacteria using some cationic thiol surfactants and their nanostructures. Am J Biochem, 2(3), 29-35 (2012).
[51] Belova, V., Möhwald, H., & Shchukin, D. G. Sonochemical intercalation of preformed gold nanoparticles into multilayered clays. Langmuir, 24(17), 9747-9753 (2008).
[52] Radwan, A. M., Hamad, M. A., & Singedy, A. M. Synthesis gas production from catalytic gasification of saw dust. Life Sci J, 12, 104-18. (2015).
[53] Featherstone, P. J., Ball, C. M., & Westhorpe, R. N., The evolution of the polyvinyl chloride endotracheal tube. Anaesth. Intensive Care Med.”. 43(4), 435-436 (2015).

[54] Ahmad, I., Khan, M. I., Khan, H., Ishaq, M., Tariq, R., Gul, K., & Ahmad, W. Pyrolysis study of polypropylene and polyethylene into premium oil products. Int. J. Green Energy 12(7), 663-671 (2015).
[55] Demirbas, A., Pyrolysis of municipal plastic wastes for recovery of gasoline-range hydrocarbons. J Anal Appl Pyrolysis 72(1), 97-102 (2004).
[56] Puglisi, A., Mondini, S., Cenedese, S., Ferretti, A. M., Santo, N., & Ponti, A. Monodisperse octahedral α-MnS and MnO nanoparticles by the decomposition of manganese oleate in the presence of sulfur. Chem. Mater 22(9), 2804-2813. (2010).
[57] Ohno, H. Science,". "Making nonmagnetic semiconductors ferromagnetic,", 281, 951. (1998).
[58] Wang, J., Wang, S., Xin, Q., & Li, YPerspectives on water-facilitated CO 2 capture materials. J. Mater. Chem A, 5(15), 6794-6816. (2017).
[59] Jeong, Y. U., & Manthiram, A. Nanocrystalline manganese oxides for electrochemical capacitors with neutral electrolytes. "J. Electrochem. Soc.".149(11), A1419. (2002).
[60] Li, X., Li, D., Qiao, L., Wang, X., Sun, X., Wang, P., & He, D. Interconnected porous MnO nanoflakes for high-performance lithium ion battery anodes. J. Mater. Chem.". 22(18), 9189-9194. (2012).
[61] Raymundo-Pinero, E., Khomenko, V., Frackowiak, E., & Beguin, F. Performance of manganese oxide/CNTs composites as electrode materials for electrochemical capacitors. J. Electrochem. Soc.". 152(1), A229. (2004).
[62] Tadokoro H *Structure of crystalline polymers* (Krieger Pub Co). (1979).